AIP | Review of Scientific Instruments

Twoaxis goniometer for reflectivity measurements of xray diffractors used in fusion researcha)

N. J. Peacock, R. Barnsley, A. Patel, M. O'Mullane, M. Singleton et al.

Citation: Rev. Sci. Instrum. **66**, 1175 (1995); doi: 10.1063/1.1146001
View online: http://dx.doi.org/10.1063/1.1146001
View Table of Contents: http://rsi.aip.org/resource/1/RSINAK/v66/i2
Published by the American Institute of Physics.

Related Articles

Diagnostics of underwater electrical wire explosion through a time- and space-resolved hard x-ray source
Rev. Sci. Instrum. 83, 103505 (2012)

A novel technique for single-shot energy-resolved 2D x-ray imaging of plasmas relevant for the inertial confinement fusion
Rev. Sci. Instrum. 83, 103504 (2012)

Near-coincident K-line and K-edge energies as ionization diagnostics for some high atomic number plasmas
Phys. Plasmas 19, 102705 (2012)

X-ray backlight measurement of preformed plasma by kJ-class petawatt LFEX laser
J. Appl. Phys. 112, 063301 (2012)

Time-resolved soft x-ray spectra from laser-produced Cu plasma
Rev. Sci. Instrum. 83, 10E138 (2012)

Additional information on Rev. Sci. Instrum.

Journal Homepage: http://rsi.aip.org
Journal Information: http://rsi.aip.org/about/about_the_journal
Top downloads: http://rsi.aip.org/features/most_downloaded
Information for Authors: http://rsi.aip.org/authors

ADVERTISEMENT

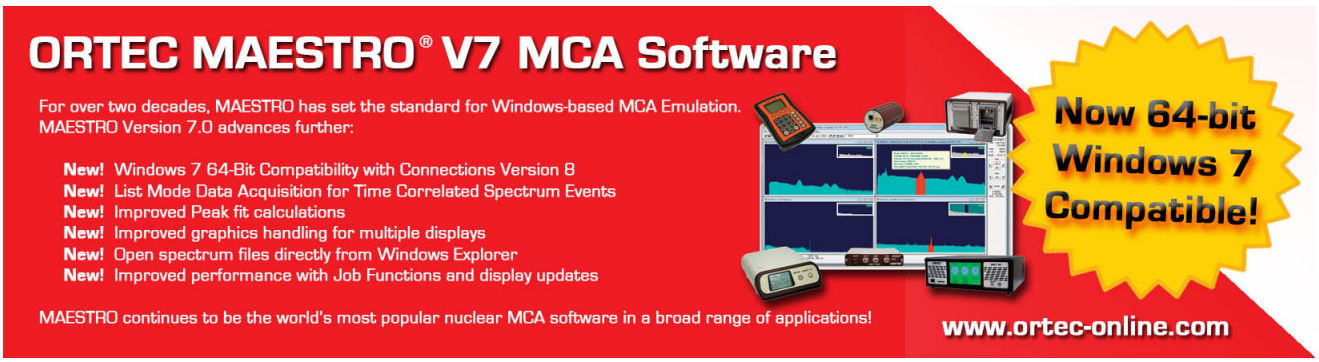

Two-axis goniometer for reflectivity measurements of x-ray diffractors used in fusion research[a)]

N. J. Peacock, R. Barnsley,[b)] A. Patel, M. O'Mullane,[c)] M. Singleton,[c)] and J. Ashall
UKAEA (Government Division, Fusion) (Euratom/UKAEA Fusion Association), Culham Laboratory, OX14 3DB, United Kingdom

(Presented on 10 May 1994)

Quantitative measurements of the line and continua emissivities and the analyses of spectral line profiles are essential steps in the interpretation of the x-ray emission from high-temperature fusion plasmas. One method of placing the emissivities on an absolute basis is to use an absolutely calibrated spectrometer to record the data. The overall sensitivity of the spectrometer can be constructed in terms of the efficiencies of its separate components, the most intractable being R_c, the reflection integral of the diffractor. To this end, a new, compact, two-axis diffractometer, incorporating modern robotic technology, such as direct-drive servomotors with closed-loop operation from built-in arcsec optical encoders, has been constructed. Improved features of this double-axis goniometer include the use of fixed line-of-sight x-ray sources with the capability of operation in the $(1,-1)$ parallel, nondispersive mode or the antiparallel, $(1,+1)$, dispersive mode. The diffractometer is now being used to calibrate x-ray diffractors, filters, mirrors, and detectors associated with x-ray spectroscopy of fusion plasmas. At certain wavelengths, where line branching ratios involving visible transitions are available, the fusion plasma may itself be used as a transfer standard of x-ray luminosity, allowing an independent check on the diffractometer values of R_c. Applications to the analyses of impurity concentrations in tokamaks are described while future applications of the diffractometer to radiation damage studies of x-ray and optical components [Hill *et al.*, Rev. Sci. Instrum. **63**, 5032 (1992)] used in D-T burning plasma experiments are envisaged.

I. INTRODUCTION

In tokamak plasmas, the radiated power loss from nonfuel ions can amount to between ~10% and ~100% of the input power, depending on the operating conditions. Spectroscopic studies[2,3] of the UV and x-ray line and continua emissivities are uniquely used to derive the elemental components of the total radiated power $P_{\mathrm{RAD}}(\mathrm{TOT})=\Sigma_i P_{\mathrm{RAD}}(Z_i)$ and of the effective ion charge state

$$Z_{\mathrm{eff}}=\sum_i \frac{n_i Z_i^2}{n_e}.$$

Such information is valuable in assessing the performance of the plasma, particularly where magnetic divertor fields are designed to control the impurity content in the core and where gettering agents (Be, B, Si, Ti, etc.) are used to reduce the oxygen content. These elements plus He, C, Cl, and metals from the vacuum vessel tend to be the most common contaminants, with emphasis on the lighter elements, particularly C. Their contributions to the total radiated power are derived from their K- and sometimes, L-shell emission in the XUV or x-ray regions (see, for example, Fig. 1). The interpretation of signal strengths from x-ray lines in terms of elemental concentrations in the plasma is something of a problem, however. The relative line strengths from the various ion species have been used with some success, when their estimated $P_{\mathrm{RAD}}(Z_i)$ contributions are normalized to the

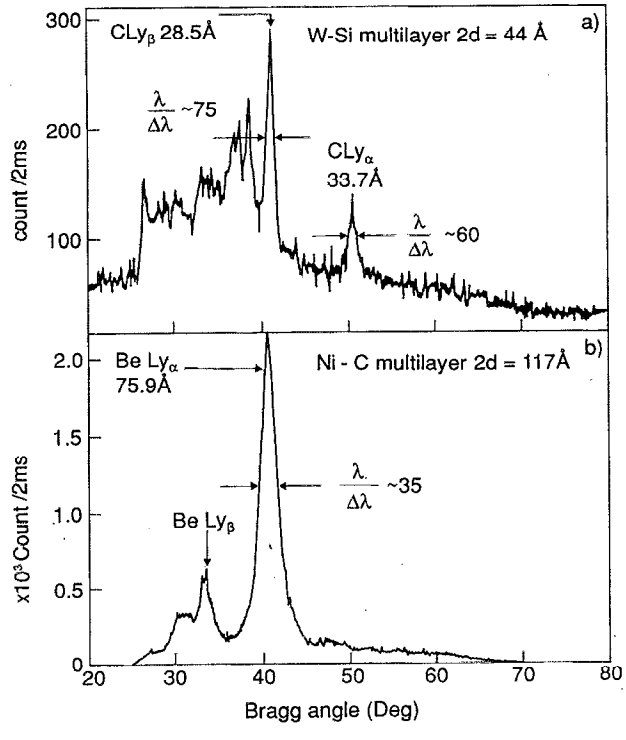

FIG. 1. Carbon and beryllium spectra recorded from the JET tokamak using (a) W-Si multilayer, $2d=44$ Å, (b) Ni-C multilayer, $2d=117$ Å.

[a)]The abstract for this paper appears in the Proceedings of the Tenth Topical Conference on High Temperature Plasma Diagnostics in Part II, Rev. Sci. Instrum. **66**, 529 (1995).

[b)]Department of Physics and Astronomy, Leicester University, LE1 7RH U.K.

[c)]University College, Cork, Ireland.

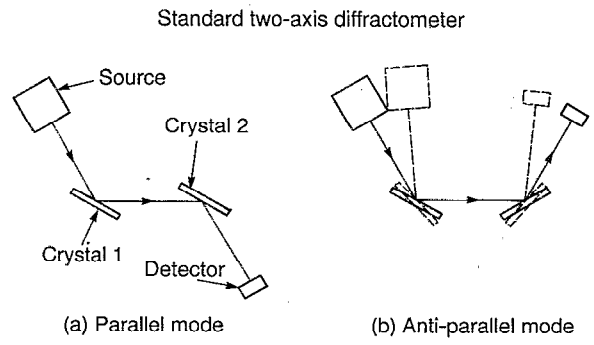

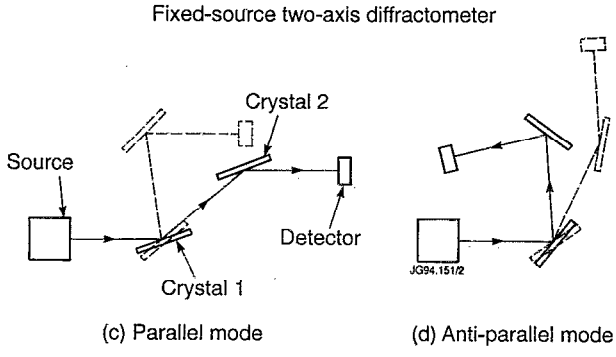

FIG. 2. Principal configurations of a two-axis diffractometer.

bolometric values of $P_{\mathrm{RAD}}(\mathrm{TOT})$.[2] A more rigorous method, however, is to measure absolute irradiances using a transfer standard of x-ray luminosity such as a synchrotron.[4] Transfer standards are notoriously awkward to use due to polarization and *f*/number mismatch with the plasma source. Ideally, the plasma source itself should be the transfer standard and as we shall see, using branching line ratios, this is sometimes possible. In this paper we opt for the construction of the overall absolute sensitivity of the spectrometer from the efficiencies of the separate components. This has been done for grating spectrometers[5] where the main problem is diffraction grating efficiency. Analogously, we focus on the problem of diffractor efficiency. One possibility is to use an extended x-ray vacuum anode source *in situ* to simulate the plasma[6,7] but this suffers from the disadvantage that the spectral bandwidth is, to some small extent, indeterminate due to the presence of background continuum. In the two-axis reflection technique adopted here, the first diffractor provides a near monochromatic illumination of the second diffractor, whose integrated reflection efficiency is independent of the source bandwidth, provided that the diffractor properties do not change over small (~0.1°) changes in the Bragg angle.

II. DIFFRACTOR CONFIGURATIONS

The different optical configurations used in a two-axis diffractometer are illustrated in Fig. 2. In the parallel mode the diffractometer analyzes the diffractor characteristics, while the antiparallel, dispersive mode analyzes the source spectral intensity. Alternating diffractor "2" between the two modes gives diffraction angle differences of $(\pi\text{-}2\theta)$ and hence the lattice spacing. In most conventional two-axis systems, the locations of the axes are fixed in space with the

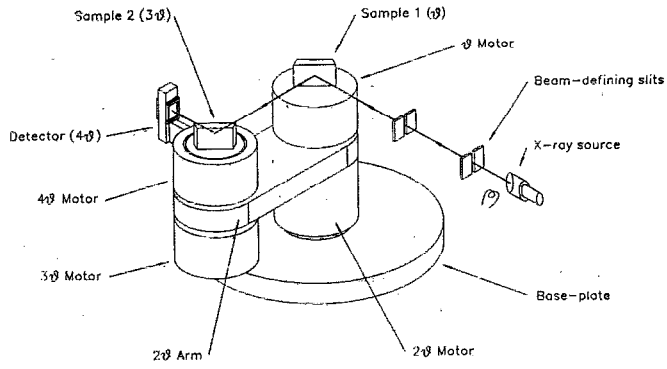

FIG. 3. Schematic of two-axis diffractometer with fixed position for the x-ray source.

source and detectors on swinging arms, preserving the $\theta \leftrightarrow 2\theta$ relation, where θ is the Bragg angle. The main advantage of the system adopted here[8] is that the source to diffractor "1" optical axis remains fixed while the second axis of the goniometer is free to rotate around the first, Figs. 2(c) and 2(d), thus making a versatile instrument where the source can be readily changed. One disadvantage of a two-axis diffractor is that the single-crystal diffraction integral,

$$R_c = \int_0^{\pi/2} P(\theta)\, d\theta,$$

where $P(\theta)$ is the intensity, or Prins function, of the diffraction profile, is not measured directly, but has to be derived

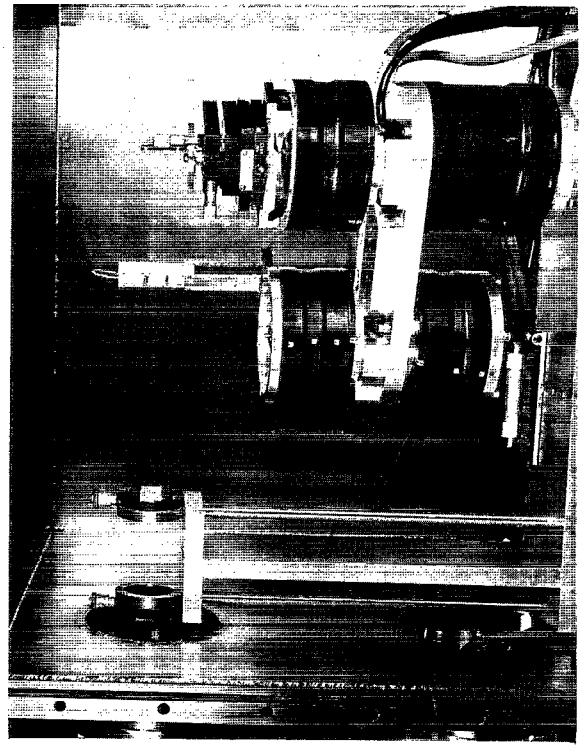

FIG. 4. Photograph of direct drive motors used in the two-axis configuration inside the diffractometer vacuum chamber.

from the measured two-crystal reflection integral, after taking into account polarization changes imposed by the first diffractor. Thus,

$$R_{cc}=2R_c\frac{1+k^2}{(1+k)^2},$$

where $k(\theta)=R_{c\pi}/R_{c\sigma}$ is the polarization ratio which can be estimated or minimized by using low Bragg angles at the first diffractor.[9] In practice, R_{cc} is measured from $R_{cc}=E\omega/I_0$, where E is the integrated counts on the detector, while scanning diffractor "2," with a rate of change of $\theta=\omega$. The bandwidth of I_0, the incident intensity onto diffractor "2," is, of course, much smaller than the detector resolution. For analyses of the plasma emission line shapes in terms of plasma ion temperature and plasma fluid motion, measurements of R_c are not enough and only accurate measurements of $P(\theta)$ at the arcsec level will suffice. The goniometer described here is well capable of this accuracy.

III. DESCRIPTION OF TWO-AXIS GONIOMETER

The two-axis goniometer employs direct drives, greatly simplifying the design and operation of the rotary tables. The mass production of these motors for industrial use has resulted in a large cost saving over specialized systems designed only a few years ago.[6] The main mechanism, as shown schematically in Fig. 3 and by the photograph in Fig. 4, consists of a base, mounted onto which are four direct-drive motors, two on each axis, with an interaxial connecting plate. The motors are positioned to about 2 arcsec by closed-loop feedback from built-in optical encoders. Crystal holders and the detector are provided with translation, rotation, and tilt mechanisms. The whole assembly provides all the motions required to achieve the configurations shown in Figs. 2(c) and 2(d). The detector is a single-wire gas proportional counter with windows back and front and is able to access Bragg angles up to 85°. The vacuum diode, x-ray sources are either conventional, 5–50 keV, sealed-off tubes giving K- and L-shell lines from the common metals or a demountable source[10] for low energies (<5 keV). The control system (by

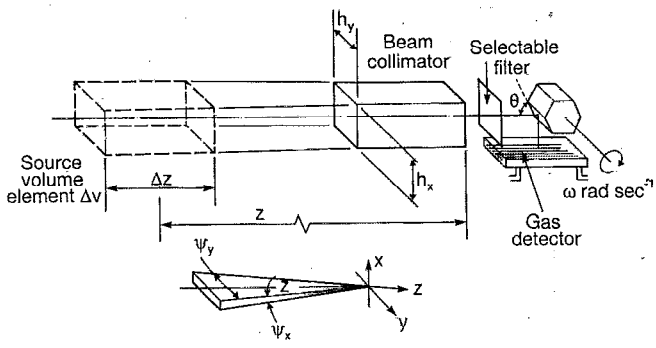

FIG. 5. Optical ray diagram of Bragg rotor spectrometer.

Micromech Ltd., U.K.) for the motor drives requires only an RS232 link from a PC to control the drives, using a high-level command language.

IV. OVERALL SENSITIVITY OF (BRAGG) SPECTROMETER

We illustrate the use of the diffractometer by constructing the absolute sensitivity of a flat crystal, x-ray survey spectrometer, the Bragg Rotor,[11,12] commonly used at the Culham Laboratory and JET (see, e.g., Fig. 1). This spectrometer has the advantage of readily accommodating flat synthetic multilayers, Langmuir–Blodgett films, and other diffractors suitable for long wavelength, $\lambda>20$ Å, diffraction.[13] The essential elements required to calculate the integrated signal, in counts, when scanning through a typical plasma x-ray line are illustrated in Fig. 5. The integrated count in scanning a line is

$$N=\epsilon(\lambda)\Delta z\frac{\Psi_x}{\omega}R_c\frac{\Psi_y}{4\pi}h_xh_y\eta_s\eta_\lambda, \quad (1)$$

where the symbols are explained in Table I. As an example, we consider the Al XII "w" resonance transition at 7.757 Å, due to "laser blow-off" injection in the COMPASS-D tokamak. The effective count rate, with no additional absorbers, peaks at 6.25 MHz using an EDDT crystal rotating at 3 Hz.

TABLE I. Breakdown of terms in Eq. (1) giving estimates of count rate.

Component	Description	Value
N: Integrated counts for Al XII line at 7.757 Å		1.56×10^3
$\epsilon(\lambda)\Delta z$: line irradiance	SANCO ion diffusion model	1.4×10^{13} photons/s cm^2
ψ_x: collimator acceptance angle in plane of dispersion	Resolving power	0.002 rad. (1:500)
ω: rate of change of Bragg angle	$2\pi f$	6π rad/s
R_c: integrated reflectivity of diffractor	EDDT (020) 2D=8.808 Å	7×10^{-5} rad (Ref. 14)
ψ_y: collimator acceptance angle perp. to dispersion	sight tube f/number	0.05 rad.
h_x: projected height of crystal at collimator		2.25 cm
h_y: projected width of crystal at collimator	sight-tube clearance	1.8 cm
η_s: transmission of structural elements		0.58 net
η_λ: efficiency of windows and detector		0.82 net

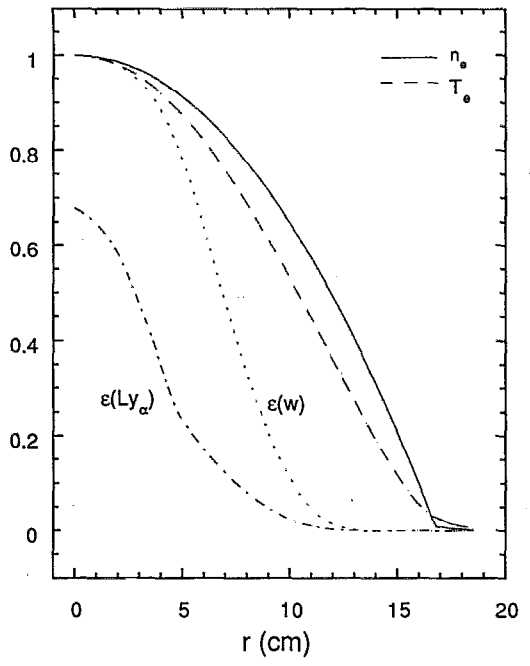

FIG. 6. Ion diffusion model (SANCO) of aluminum ion emission in the COMPASS-D tokamak. $\hat{T}_e(0)=1$ keV, $\hat{n}_e(0)=6.6\times10^{19}$ m^{-3}. The irradiance $\epsilon(\lambda)\Delta z$ of Al XII "w" line is 1.4×10^{17} photons m^{-2} s^{-1}. The Al XII Ly$_\alpha$ volume emissivity is also shown (normalized to "w" line).

The factor R_c has not been measured using the present diffractometer, but has been taken from a previous two-axis goniometer study of EDDT at Leicester University.[14] The count rate is mainly dependent on the electron density n_e and the Al ion density in the core plasma. The irradiance of the line, $\epsilon(\lambda)\Delta z$, is generated using the SANCO ion diffusion

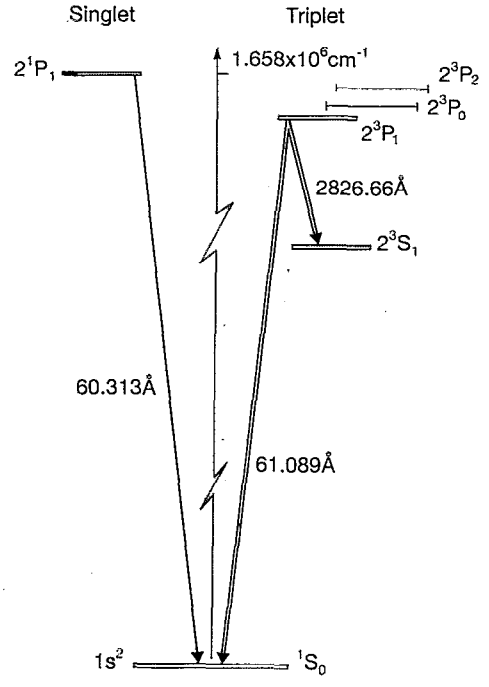

FIG. 7. Term scheme of B IV.

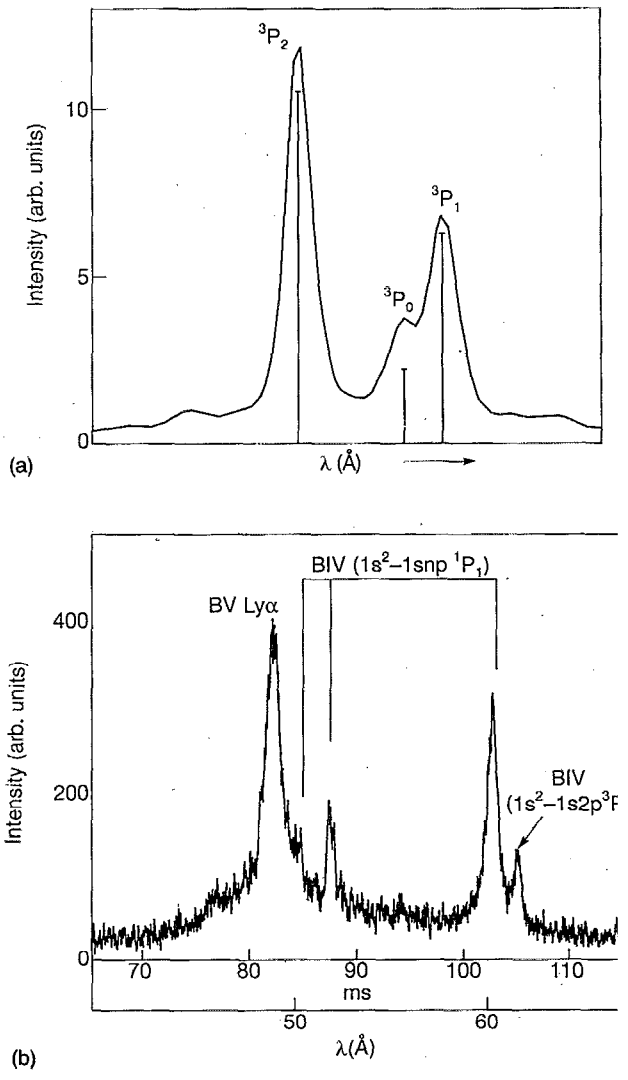

FIG. 8. (a) Spectrum of the B IV $1s2s\ ^3S_1-1s2p\ ^3P_{0,1,2}$ multiplet 2825.36, 2826.66, and 2822.46 Å from the COMPASS-D tokamak. Bragg Rotor spectrum of B IV and B V from the COMPASS-D tokama

code with established diffusive and convective paramete and the COMPASS $T_e(r)$ and $n_e(r)$ radial distributions, F 6. We adopt a parameter $\langle n_e(r=0)N[\mathrm{AlXII}(r=0)]\rangle$ as main quantity Q determining the count rate. The Bragg sp trometer gives a value of $Q=3.27\times10^{23}$ cm^{-6}, in agr ment with estimates derived from the Si(Li) detec spectrum.[15]

V. ABSOLUTE CALIBRATION USING BRANCHING RATIOS

Branching ratios, see, e.g., Fig. 7, from the $1s2p\ ^3$ common, upper level in He-like ions of the light eleme Be, B, and C are attractive candidates for establishi absolute line irradiances from fusion plasmas in the s x-ray region.[16] The long-wavelength brar ($1s2s\ ^3S_1-1s2p\ ^3P_1$) lies in the near visible, where fil optics transmission is possible and where the line intens can be calibrated against a standard lamp. For B IV, branching ratio A(2826.66 Å)/A(61.089 Å) is 11/1. The lo wavelength component is well separated from the neighb

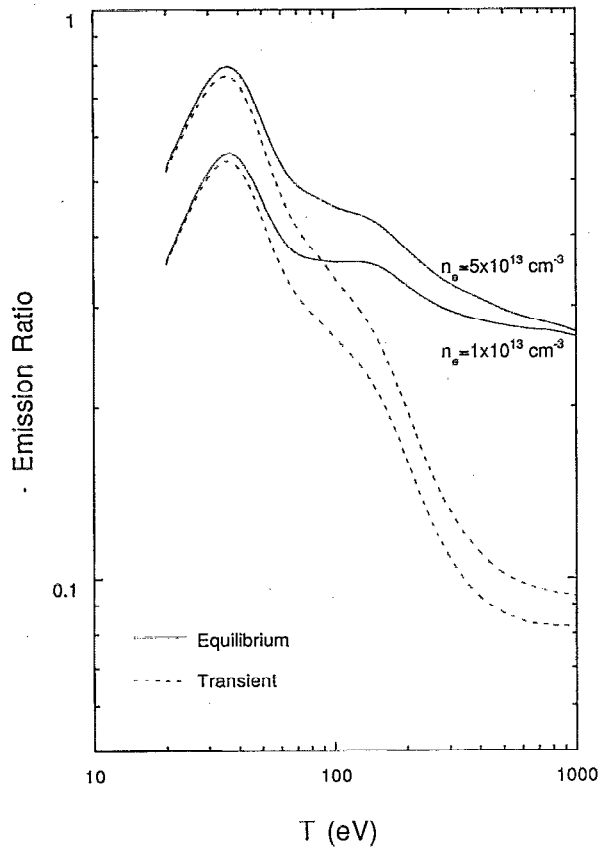

FIG. 9. Model calculation of the ratio of $1s^2-1s2p\ ^3P_1/1s^2-1s2p\ ^1P_1$ transitions in B IV.

ing components of the triplet with even a modest resolution (0.6 m Spex spectrometer), while the short wavelength ($1s^{21}S_1-1s2p^3P_1$) is readily resolved from the parent ($1s\ ^2S_1-1s2p\ ^1P_1$) line using an OHM crystal as shown by the data from the COMPASS-D tokamak in Figs. 8(a) and 8(b). Typically, in these plasma experiments, the intensity ratio (I_i/I_a) of the intercombination to allowed x-ray lines lies in the range 0.1–0.3, depending on plasma parameters, Fig. 9. The B IV emission is predominantly from transient, i.e., rapidly diffusing, ions about 4 cm inboard of the plasma edge where $T_e \leqslant 200$ eV. In the case where the 61.089 Å line is obscured in the noise level, the parent line at 60.31 Å may be used as a secondary standard, provided that (I_i/I_a) is well established over a set of similar tokamak discharges.

VI. CONCLUSIONS

The overall sensitivity of a flat crystal spectrometer has been constructed from the reflection integral of the diffractor R_c and other geometric and efficiency factors. The spectrometer efficiency is in reasonable agreement with the observed count rates expected from model calculations of the absolute x-ray line emissivities from the COMPASS-D tokamak. The immediate use of the two-axis goniometer will be to check R_c for OHM crystals and to compare the absolute spectrometer sensitivity with that derived from branching ratios. In the longer term, the goniometer will be used for R_c measurements of synthetic multilayer diffractors and mirrors now being considered for D-T fusion experiments.

[1] K. W. Hill, K. M. Young, M. Bitter, S. von Goeler, H. Hsuan, R. Hulse, L.-P. Ku, and B. C. Stratton, Rev. Sci. Instrum. **63**, 5032 (1992).

[2] K. D. Lawson, R. Barnsley, R. Gianella, N. Gottardi, N. C. Hawkes, F. Montpean, T. K. Patel, and N. J. Peacock, Proceedings of the 17th EPS Conference on Controlled Fusion and Plasma Physics, Amsterdam June 1990, Europhys. Conf. Abstracts **14B**, 1413 (1990).

[3] K. D. Lawson, R. Barnsley, R. Gianella, L. Lauro-Taroni, M. G. O'Mullane, N. J. Peacock, and P. Smeulders, Proceedings of the 20th EPS Conferences on Controlled Fusion and Plasma Physics, Lisbon, July 1993. Europhys. Conference Abstracts Vol. **17C**, paper 1.13 (1993).

[4] A. P. Zwicker, M. Finkenthal, L.-K. Huang, S. P. Regan, M. J. May, and H. Warren Moos, Rev. Sci. Instrum. **63**, 5035 (1992).

[5] M. G. Hobby and N. J. Peacock, J. Phys. E **6**, 854 (1973).

[6] H. W. Morsi, H. Röhr, and U. Schumacher, Z. Naturforsch. Teil A **42**, 1051 (1987).

[7] R. Barnsley, U. Schumacher *et al.*, Rev. Sci. Instrum. **62**, 889 (1991).

[8] R. Barnsley, Ph.D. thesis, University of Leicester, 1993.

[9] K. D. Evans and B. Leigh, Space Sci. Instrum. **2**, 105 (1976).

[10] B. B. Jones and Freeman, Conference on Calibration Methods in the UV and X-ray Region of the Spectrum, ESRO (Geneva) SP-33, pp. 245–52 (1968).

[11] R. Barnsley, S. N. Lea, A. Patel, and N. J. Peacock, in *UV and X-ray Spectroscopy of Laboratory and Astophysical Plasmas*, edited by E. Silver and S. Khan (Cambridge University, Cambridge, 1993), p. 514.

[12] R. Barnsley, J. Brzozowski, I. H. Coffey, K. D. Lawson, A. Patel, T. K. Patel, N. J. Peacock, and U. Schumacher, Rev. Sci. Instrum. **63**, 5023 (1992).

[13] A. P. Zwicker, S. P. Regan, M. Finkenthal, H. Warren Moos, Ed. B. Saloman, R. Watts, and J. R. Roberts, Appl. Opt. **29**, 3694 (1990).

[14] R. Hall, Ph.D. thesis, University of Leicester, 1980.

[15] J. Ashall, Internal Note Compass(94) N10, UKAEA Fusion, The Culham Laboratory, 1994.

[16] N. C. Hawkes, K. D. Lawson, and N. J. Peacock, in *UV and X-ray Spectroscopy of Laboratory and Astophysical plasmas*, edited by E. Silver and S. Khan (Cambridge University, Cambridge 1993), p. 324.